Supporting information

Catalytic Silylation of Dinitrogen by a Family of Triiron Complexes

Ricardo Ferreira[†], Brian J. Cook[†], Brian J. Knight[†], Vincent J. Catalano[‡], Ricardo García-Serres,[§] and Leslie J. Murray[†,*]

[†] Center for Catalysis and Florida Center for Heterocyclic Chemistry, Department of Chemistry, University of Florida, Gainesville, FL 32611, USA
[‡] Department of Chemistry, University of Nevada, Reno, NV 89557, United States
[§] Université Grenoble Alpes, CNRS, CEA, BIG, LCBM (UMR 5249), F-38054 Grenoble, France

*Correspondence: murray@chem.ufl.edu

Table of Contents

Experimental Section

General Considerations. All manipulations were carried out inside a N_2-filled Innovative Technologies glovebox unless otherwise stated. Tetrahydrofuran (THF), benzene, toluene, *n*-hexane, and diethyl ether were purchased from Sigma-Aldrich, then purified through drying columns from Innovative Technologies solvent purification system, and stored over activated 3 Å molecular sieves. Dimethylsulfoxide-d_6 (DMSO-d_6) was purchased from Cambridge Isotope Laboratories and used without further purification. C_6D_6 was purchased from Cambridge Isotope Laboratories, dried over CaH_2 under reflux, then distilled and degassed and stored over 3 Å molecular sieves. Fe_3Br_3**L**, Fe_3X_3**L** (X = H, F, S), $Fe_3H_2(HCOO)$**L**, $(FeCO)_2Fe(\mu_3\text{-}H)$**L**, $Fe_3Br_2(\mu_3\text{-}N)$**L**, and $[FeCl\mathbf{L'}]_2$ were synthesized as reported previously.[1–6]

^{1}H Nuclear Magnetic Resonance (^{1}H NMR) spectra were recorded on a Varian Inova 500 MHz spectrometer or a Mercury operating at 300 MHz equipped with a three-channel 5 mm indirect detection probe with z-axis gradients. Chemical shifts were reported in δ (ppm) and were referenced to solvent resonances δ_H = 7.16 ppm and 2.50 ppm for benzene-d_6 and dimethylsulfoxide-d_6, respectively. FT-IR spectra were collected on drop-casted samples using a ThermoFisher Scientific Nicolet iS5 spectrometer equipped with an iD7 ATR stage and using the OMNIC software package at 1.0 cm-1 resolution and 32 scans per sample. Mass spectrometry data were collected using an Agilent 6220 ESI-TOF on samples prepared in THF or MeCN at analyte concentrations of 16.0 μM. Gas chromatography was performed using a Shimadzu GC-2014 instrument equipped with a Quadrex fused silica capillary column (Methyl 5% Phenyl Silicone, length: 30 m, inner diameter: 0.25 mm, film thickness: 0.25 μm). The instrument.

Reductions of Fe_3Br_3L with 3 or 6 equivalents of KC_8. Fe_3Br_3**L** (20.0 mg, 18.2 μmol) was combined with 3 or 6 equivalents of KC_8 as solids and cooled down to -34 °C. To the solids, 8 mL of the desired solvent (toluene, THF, or Et_2O) was added at -34 °C under stirring using a glass stirbar. The mixture was kept at -34 °C under stirring for 16 h, then filtered over a Nylon membrane in which the black residue was washed with 2 mL of the corresponding solvent. The combined amber filtrate was evaporated under reduced pressure to afford brown solids that were assessed by ^{1}H-NMR.

Stoichiometric reductions of triiron complexes with 6 equivalents of KC_8. In a typical experiment, triiron complex (22.0 μmol) was combined with 6 equivalents of KC_8 as solids at ambient temperature To the solids, toluene (3.4 mL) and then 6 equivalents of Me_3SiCl was added under stirring using a glass stirbar. The mixture was kept at ambient temperature under stirring for 24 h, and then the mixture was filtered through a toluene rinsed plug. The combined amber filtrate was evaporated under reduced pressure and was assessed by ^{1}H-NMR.

Catalytic N_2 silylation to tris(trimethylsilyl)amine using Fe_3Br_3L. KC_8 (45.0 mg, 333 μmol) was suspended in 1.80 mL of the desired solvent (toluene, THF, or diethyl ether) under stirring with a glass stirbar. To this slurry, chlorotrimethylsilane (Me_3SiCl, 42.2 μL, 333 μmol) was added followed by 0.200 mL of a 3.3 mmol L^{-1} solution of Fe_3Br_3**L** in toluene. The system was kept at room temperature for 24 h, then filtered to afford a clear filtrate. The presence of $N(SiMe_3)_3$ in the filtrate was confirmed by gas chromatography (Figure S11). To the filtrate, 0.100 mL of a 4 mol L^{-1} HCl solution in 1,4-dioxane was added and, after 5 min, volatiles were removed to afford white solids. The resulting solid was dissolved in dimethylsulfoxide-d_6 with 1,3,5-trimethoxybenzene as an internal standard to quantify ammonium. The experiments were performed in triplicate for the values presenting an error bar.

Filtration experiments. KC_8 (11.2 mg, 83.2 μmol) was suspended in 1.80 mL of the desired solvent (toluene or diethyl ether) under stirring with a glass stirbar. To this slurry, Me_3SiCl (10.5 μL, 83.2 μmol) was added followed by 0.200 mL of a 3.3 mmol L^{-1} solution of Fe_3Br_3**L** in toluene. The system was kept at room temperature for 6 h, then filtered to afford a dark residue and a pale yellow filtrate. To the isolated residue and filtrate, KC_8 (33.8 mg, 250 μmol) and Me_3SiCl (31.5 μL, 250 μmol) were added. To the residue, 1.80 mL of the desired solvent was also combined. Both systems were kept under stirring at room temperature for an extra 18 h. Ammonium was quanti-

fied as described above. In toluene, the filtrate and residue resulted in 25 and 7 NH_4^+ equiv./Fe, respectively (22% of heterogeneous activity). In diethyl ether, the filtrate and residue resulted in 64 and 10 NH_4^+ equiv./Fe, respectively (13% of heterogeneous activity).
The same procedure was followed with an equimolar amount of iron as [FeCl**L'**]$_2$. In toluene, the filtrate and residue resulted in 20 and 7 NH_4^+ equiv./Fe, respectively (26% of heterogenous activity). In diethyl ether, the filtrate and residue resulted in 37 and 19 NH_4^+ equiv./Fe, respectively (34% of heterogeneous activity).

Catalytic N_2 silylation to $N(SiMe_3)_3$ using other triiron compounds. An analogous procedure was used by using 3.3 mmol L^{-1} solutions of the desired complexes in place of the Fe_3Br_3**L** solution. The reaction was stopped after 24 h at room temperature. Ammonium was quantified as described above. The experiments were performed in triplicate.

Synthesis of $Fe_3(\mu_3\text{-}N)$L. A 20 mL scintillation vial was charged with $Fe_3Br_2(\mu_3\text{-}N)$L (300 mg, 295 μmol), 15 mL PhMe, and a Pyrex magnetic stir bar. To this was added 600 μL (0.600 mmol) KHB(*sec*-Bu)$_3$ (1.0 M in THF) and immediate effervescence was observed. The reaction was allowed to stir at room temperature for 4 h, upon which a gradual color change from dark orange-red to dark yellow-orange was observed. The reaction mixture was filtered through a Celite plug and volatiles removed under reduced pressure to yield a tacky brown solid. The solid was extracted with 2 x 5 mL n-hexane and dried under reduced pressure. The resulting solid was dissolved in the minimum amount of benzene and lyophilized to yield a brown flocculent powder. Single crystals suitable for X-ray diffraction were obtained vial slow evaporation from either a saturated benzene solution or saturated toluene solution. ^{1}H NMR (500 MHz, C_6D_6, 298 K): δ = 54.0 (s, br, 3H), 29.8 (s, 18H), 16.5 (s, br, 12H), -20.0 (s, br, 18H), -71.9 (s, br, 12 H). μ_{eff} (C_6D_6, 298 K) = 5.70 μ_B. ATR-IR (cm^{-1}) 2950(s), 2940(s), 2864(s), 1525(s), 1458(vs), 1431(s), 1399(vs), 1374(s), 1336(s), 1014(w), 929(vw), 770(vw), 735(vw).

Synthesis of Fe_3O_3L. A 50 mL Schlenk flask was charged with Fe_3H_3L (240 mg, 280 μmol), a Teflon-coated stir bar, and THF (20 mL). The solution was degassed by the freeze-pump-thaw method and then exposed to a slow flow of O_2 for 2 minutes with stirring. The flask was closed and the reaction was stirred for 2 hours. A rapid color change from dark red-orange to dark red occurring upon stirring. After this time the reaction was evaporated and the residue was dissolved in boiling toluene. Cooling the solution to -35 °C yielded dark red crystals (63.5 mg, 25%) after 2 d. ^{1}H NMR (500 MH, THF-d_8, 298 K): δ = 42.6 (12H), 6.88 (12H), 1.27 (18H), 1.19 (18H), -14.2 (3H). μ_{eff} (THF-*d_8*, 298 K) = 4.4 μB. ATR-IR (cm^{-1}): 1528, 1463, 1430, 1396, 1374, 1336, 1018, 748, 729. UV-vis (THF; nm (ε, $M^{-1}cm^{-1}$)): 315 (3.20(4) x 10^4), 405 (1.28(2) x 10^4), 545 (2.3(3) x 10^3). HRMS (ESI+) m/z calcd for ($M+H^+$) $[C_{45}H_{64}Fe_3N_6O_3]^+$: 904.3083, found 904.2939.

Synthesis of Fe_3Cl_3L. A 20 mL scintillation vial was charged with H_3L (100 mg, 145 μmol), a Teflon-coated stir bar, and THF (4.0 mL) and sealed with a Teflon-coated cap. The suspension was added BnK (60.0 mg, 0.460 mmol) at ambient temperature and stirred for 15 min. At this point, the reaction was charged with FeCl2•1.5THF (110 mg, 0.467 mmol) rapidly turning orange-red and stirred at ambient temperature for 12 h. The suspension was filtered through a plug of celite, evaporated, dissolved in benzene, and filtered through a second plug of celite. Slow evaporation of this solution yielded orange crystals (45.7 mg, 33%) after 4 weeks. The solid-state structure illustrates an idealized C_{2v} species at 100 K, while the compound is D_{3h} on the ^{1}H NMR method timescale at ambient temperature. ^{1}H NMR (C_6D_6): δ = 182 (12H), -7.98 (18H), -14.0 (12H), -43.1 (18H), -51.7 (3H). μ_{eff} (C_6D_6, 298 K) = 7.2 μ_B. ATR-IR (cm^{-1}): 1518, 1456, 1429, 1391, 1372, 1329, 1067, 1015, 733, 723 cm^{-1}. UV-vis (THF; nm (ε, M-1cm-1)): 318 (1.23(3) x 10^5), 413 (4.0(5) x 10^3). HRMS (ESI+) m/z calcd ($M+H_2O$-Cl^-) $[C_{45}H_{65}Cl_2Fe_3N_6O]^+$: 943.2640, found 943.2558.

Characterization of New Compounds

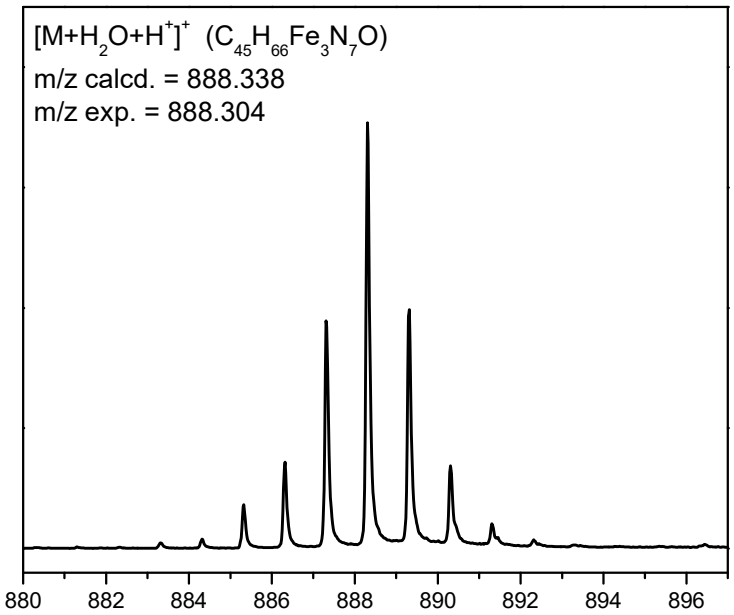

Figure S1. ESI-MS spectrum of $Fe_3(\mu_3\text{-}N)$**L** in THF (positive mode).

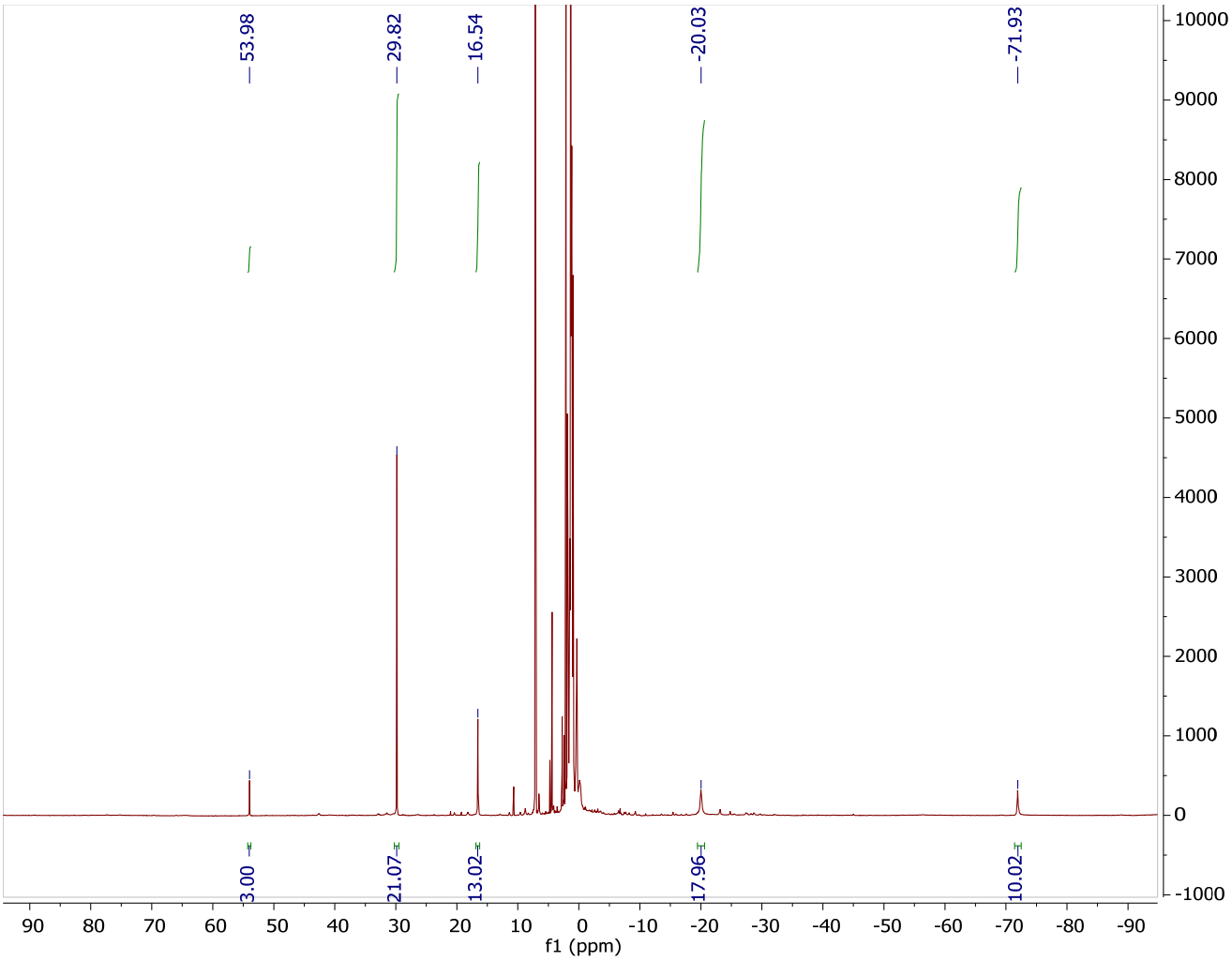

Figure S2. ^{1}H NMR spectrum of $Fe_3(\mu_3\text{-}N)$**L** in C_6D_6.

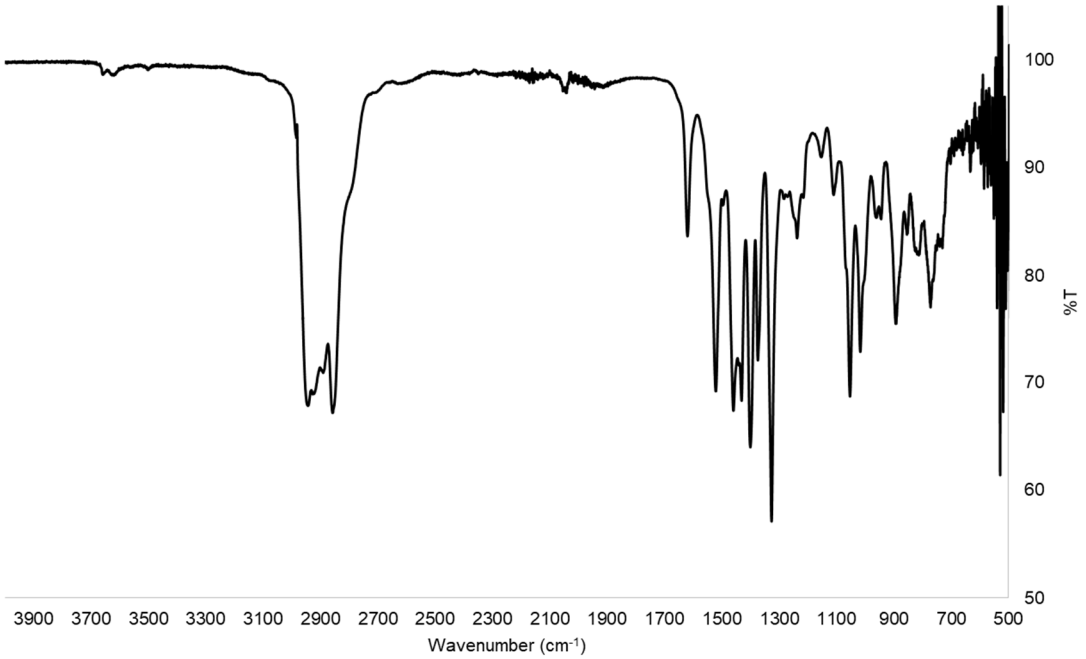

Figure S3. ATR-IR spectrum of $Fe_3(\mu_3\text{-N})$**L**, synthesized from $KHB(sec\text{-}Bu)_3$ in toluene, recorded as a thin film.

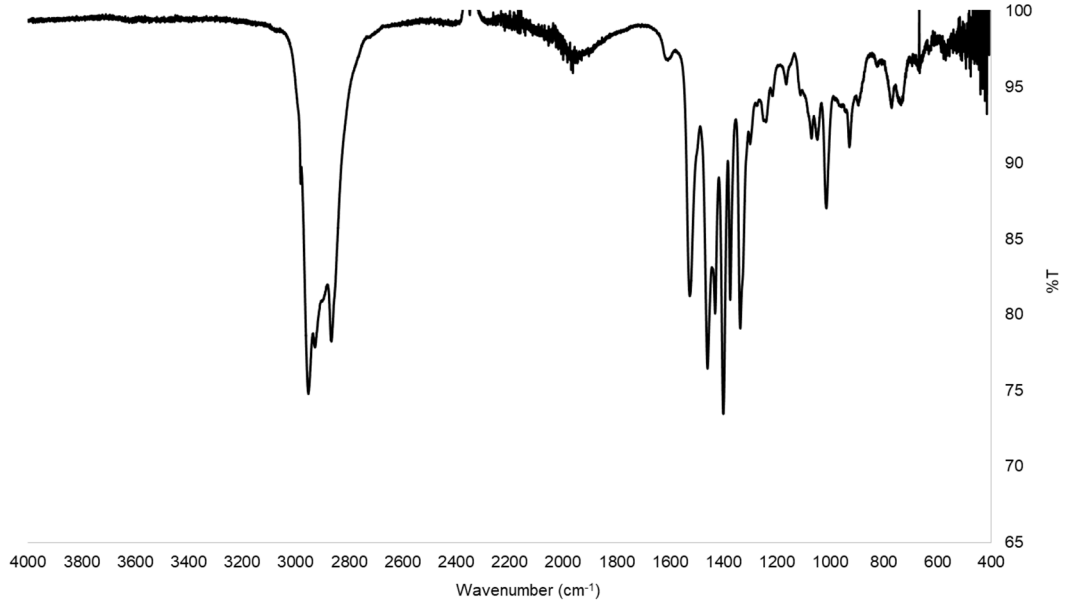

Figure S4. ATR-IR of $Fe_3(\mu_3\text{-N})$**L** synthesis from $KHBEt_3$ in toluene, recorded as a thin film.

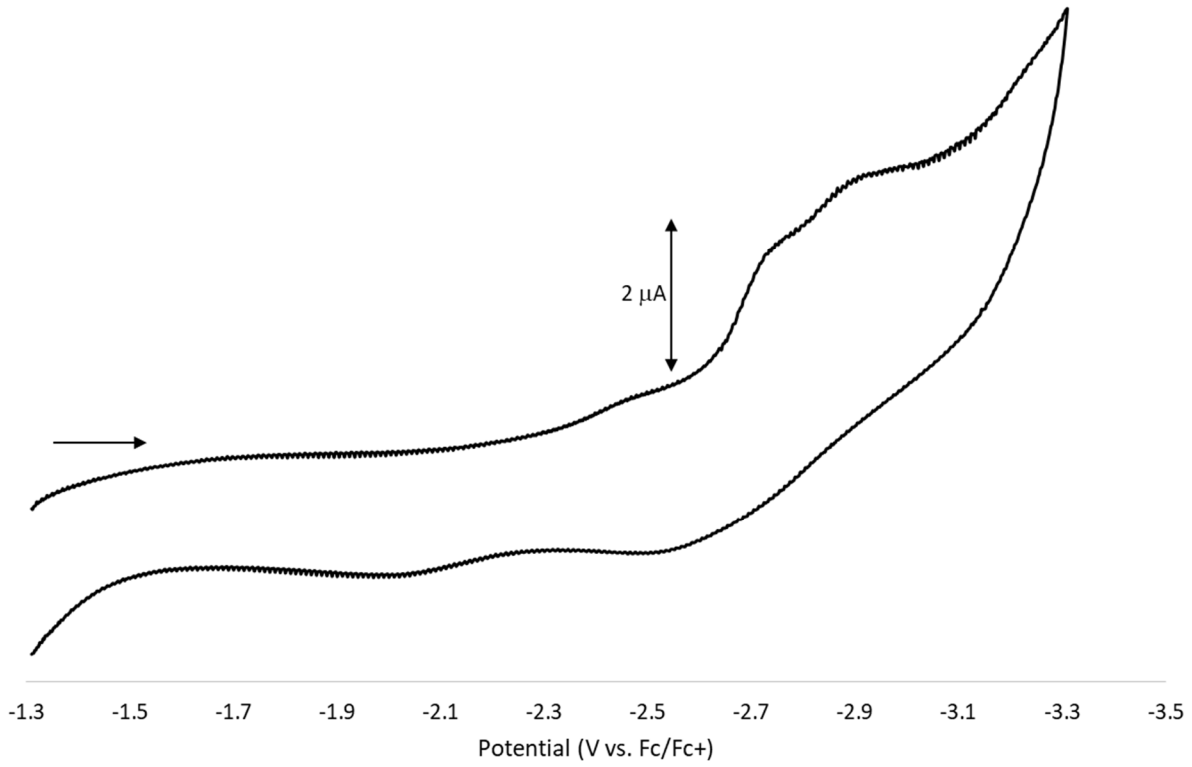

Figure S5. Cyclic Voltammetry (CV) of $Fe_3(\mu_3\text{-}N)$**L**.

Arrows indicate scan direction and origin. Working electrode: Pt button. Auxiliary Electrode: Au ribbon. Reference Electrode: Ag/AgCl wire. Analyte Concentration: 2.0 mM.

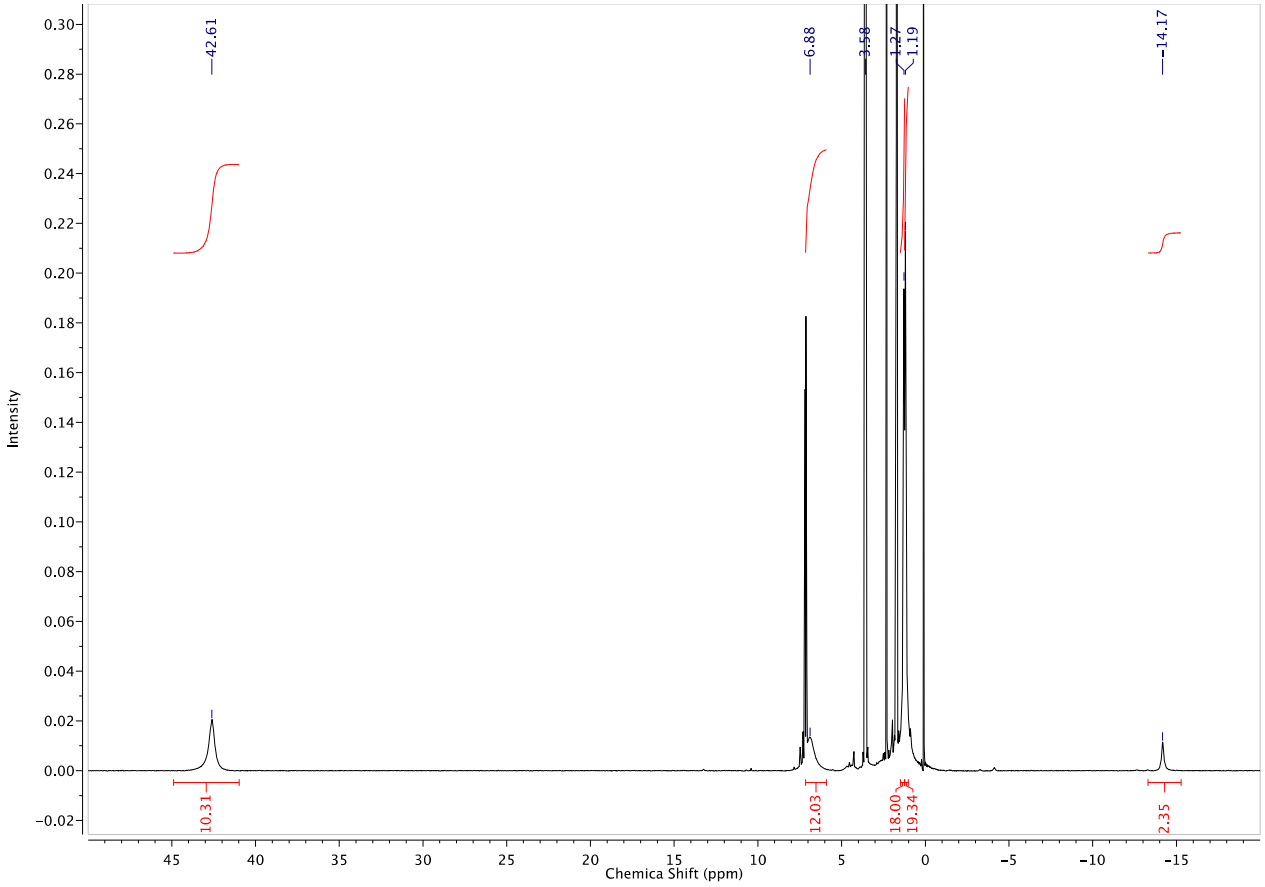

Figure S6. ^{1}H NMR spectrum of Fe_3O_3**L** in C_6D_6.

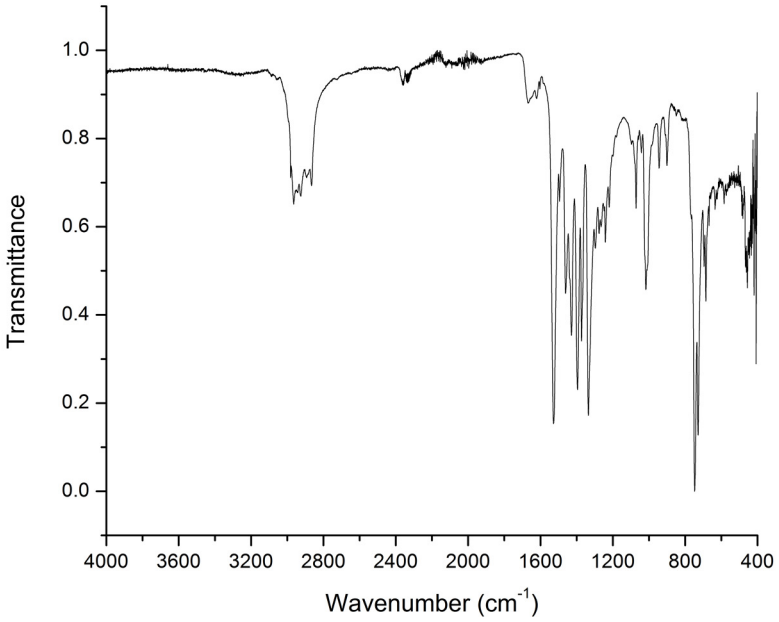

Figure S7. IR spectrum of Fe_3O_3**L**.

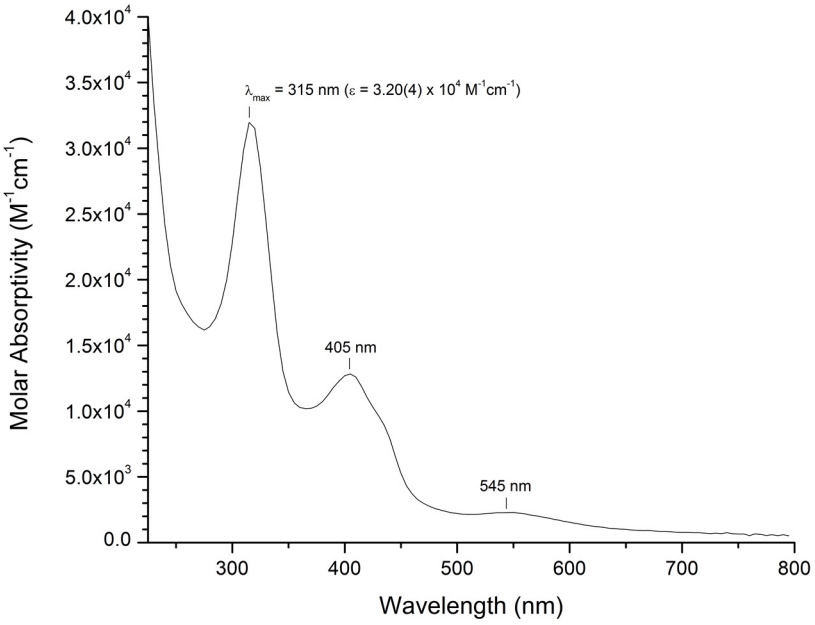

Figure S8. UV-Vis spectrum of Fe_3O_3**L** in THF.

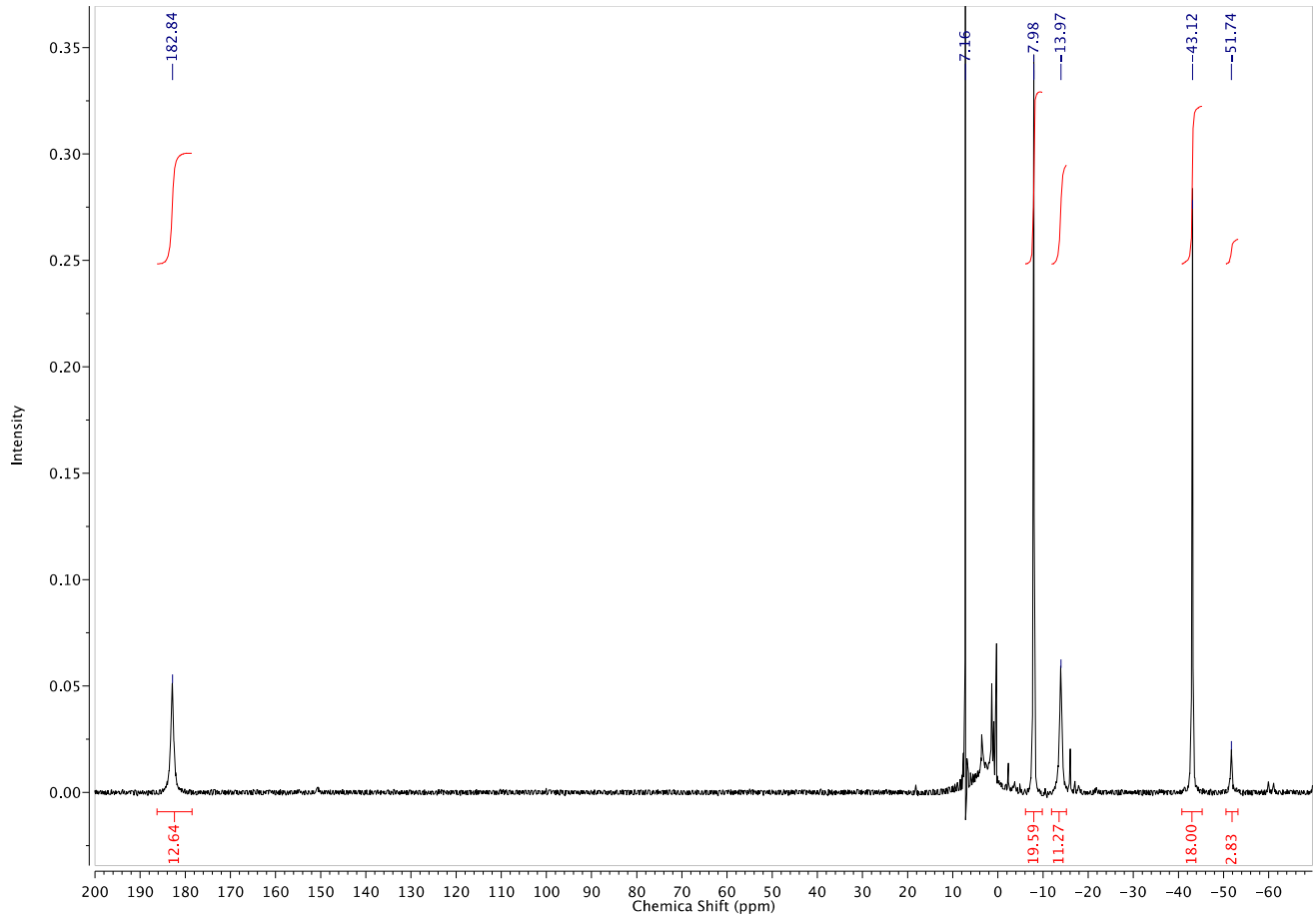

Figure S9. ^{1}H NMR spectrum of Fe_3Cl_3**L** in C_6D_6.

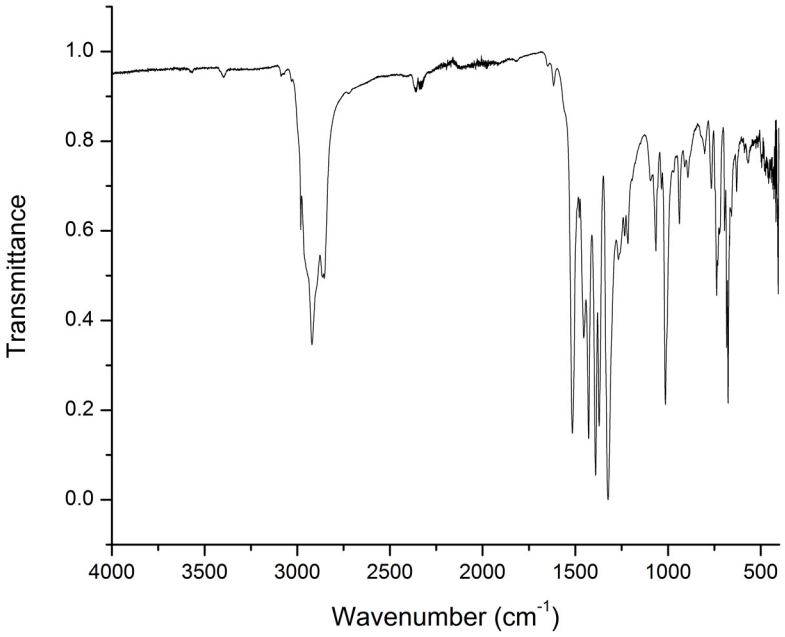

Figure S10. IR spectrum of Fe_3Cl_3**L**.

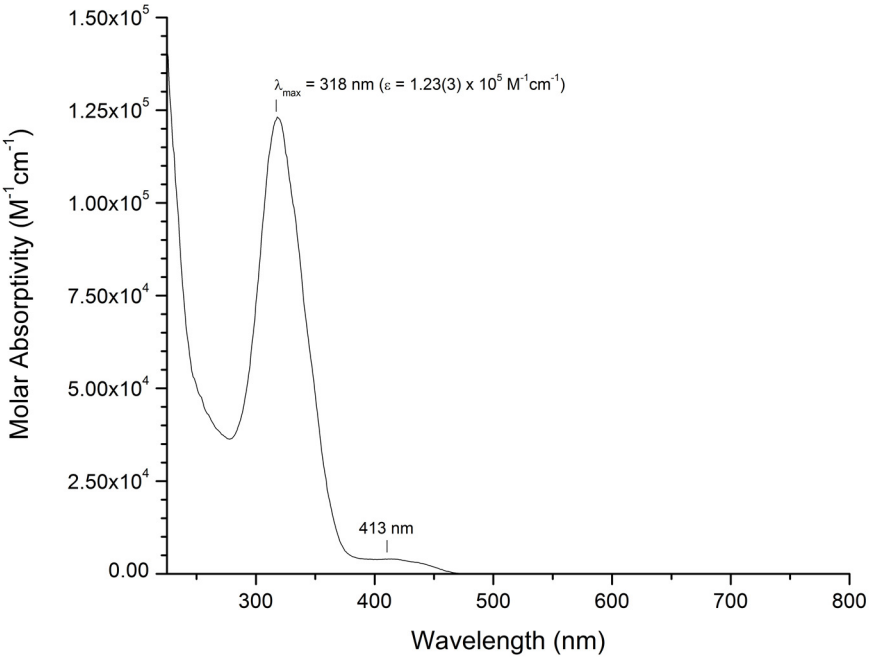

Figure S11. UV-Vis spectrum of Fe_3Cl_3**L** in THF.

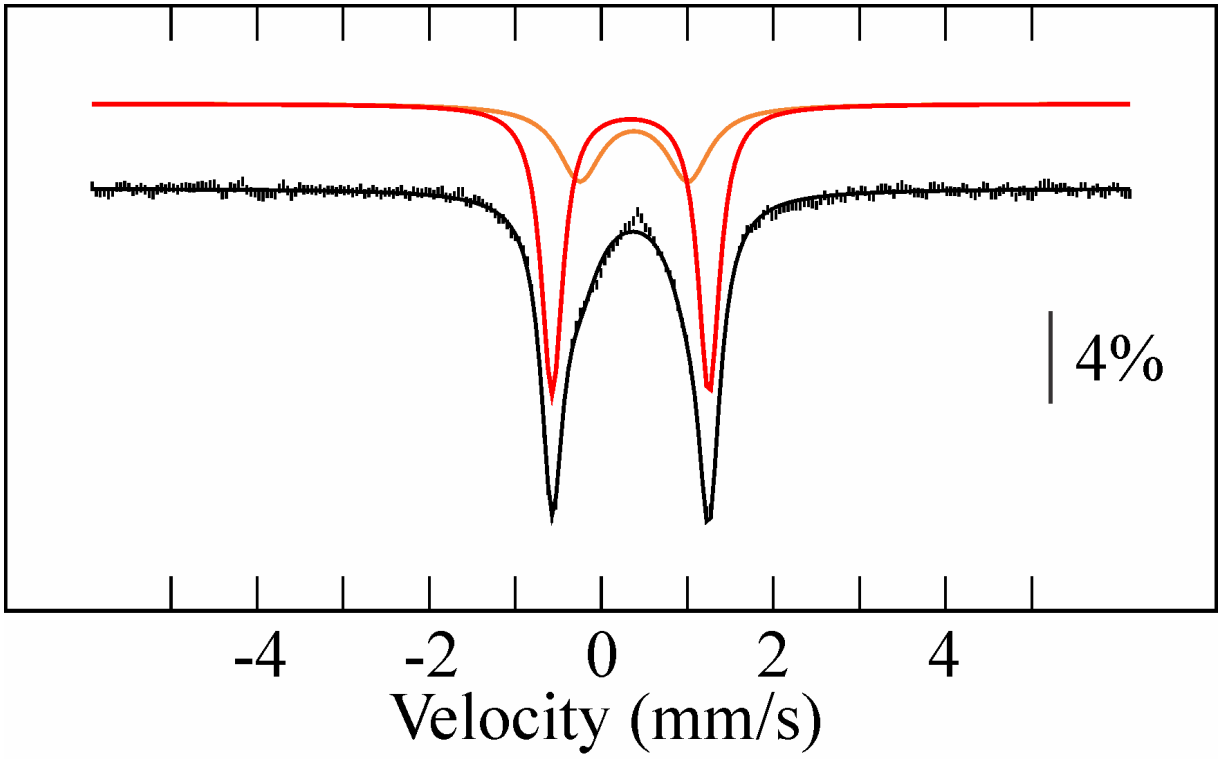

Figure S12. Mössbauer spectrum of Fe_3O_3L recorded at 80 K and zero-applied field.

Black bars and colored lines represent the experimental and simulated quadrupole doublets, respectively. Solid black line is a composite spectrum obtained by combining individual doublets. The data suggest a C_{2v}-symmetric compound by this method and on this timescale.

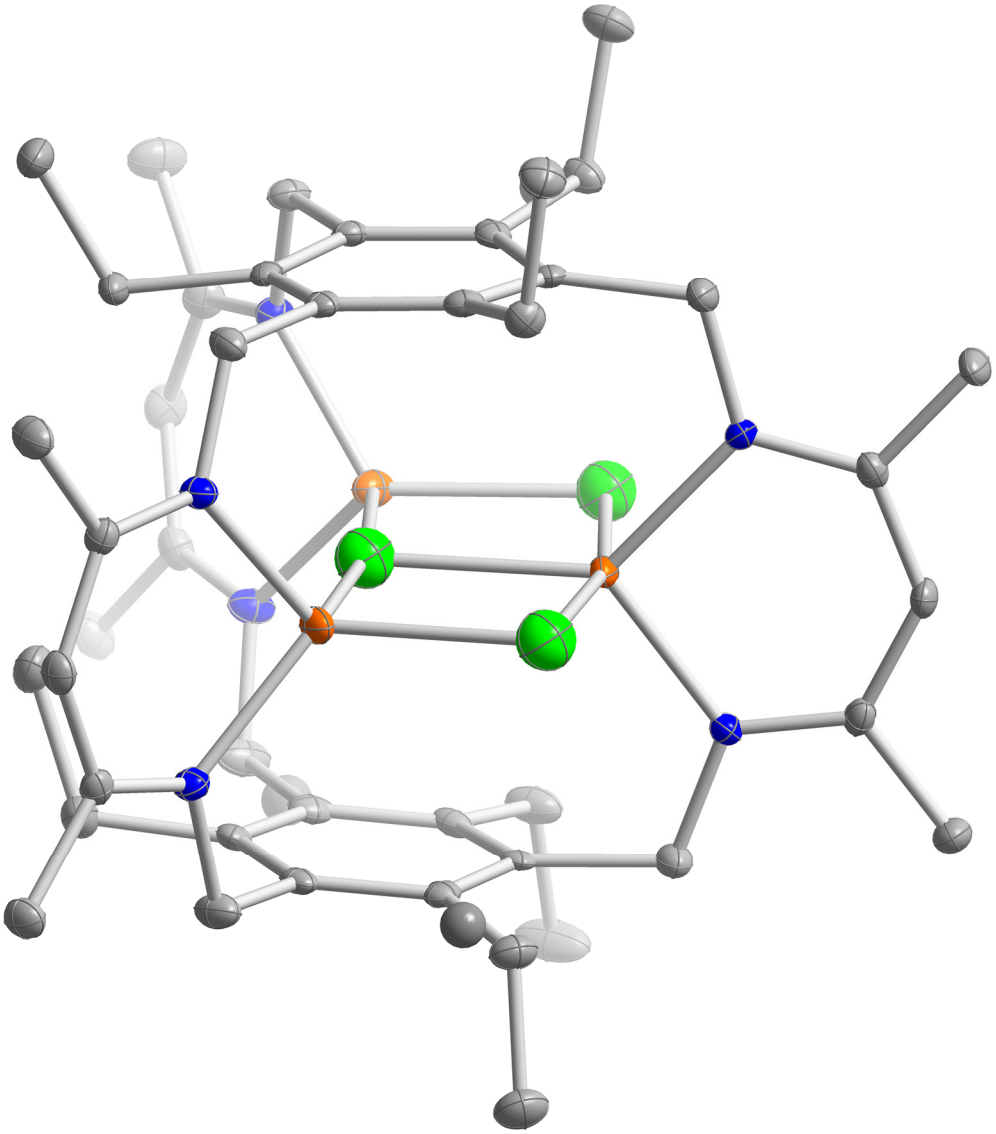

Figure S13. Single-crystal structure of Fe_3Cl_3**L** at 50% thermal ellipsoid.

The hydrogen atoms and benzene solvent molecules have been omitted for clarity. C, N, Cl, and Fe are depicted as grey, blue, green, and orange, respectively.

Table S1. 80 K Mössbauer parameters of complexes used as silylation catalysts.

complex[a]	**δ (mm/s)**	**ΔE_Q (mm/s)**	**Γ (mm/s)**	**Fe centers /3**	**Oxidation number**
Fe_3Br_3**L**	1.02	1.79	0.40	1	Fe^{II}
	0.95	2.32	0.40	1	Fe^{II}
	0.90	2.78	0.38	1	Fe^{II}
Fe_3F_3**L**	1.00	2.54	0.35	3	Fe^{II}
Fe_3H_3**L**[b]	0.77	2.26	0.35	3	Fe^{II}
$Fe_3H_2(O_2CH)$**L**[b]	0.82	2.45	0.35	2	Fe^{II}
	0.77	2.26	0.35	1	Fe^{II}
$(FeCO)_2Fe(\mu_3\text{-}H)$**L**[b]	0.66	2.60	0.31	2	Fe^{I}
	0.98	2.15	0.27	1	Fe^{II}
Fe_3O_3**L**	0.34	1.82	0.30	2	Fe^{III}
	0.38	1.26	0.60	1	Fe^{III}
Fe_3S_3**L**[b]	0.28	1.33	0.29	3	Fe^{III}

[a]We report only the complexes whose Mössbauer spectra could be entirely accounted for as the superposition of three quadrupole doublets with equal integrations, which we could confidently assign. [b]These parameters have already been reported in previous work (ESI references 3, 4, and 5).

Catalytic silylation data

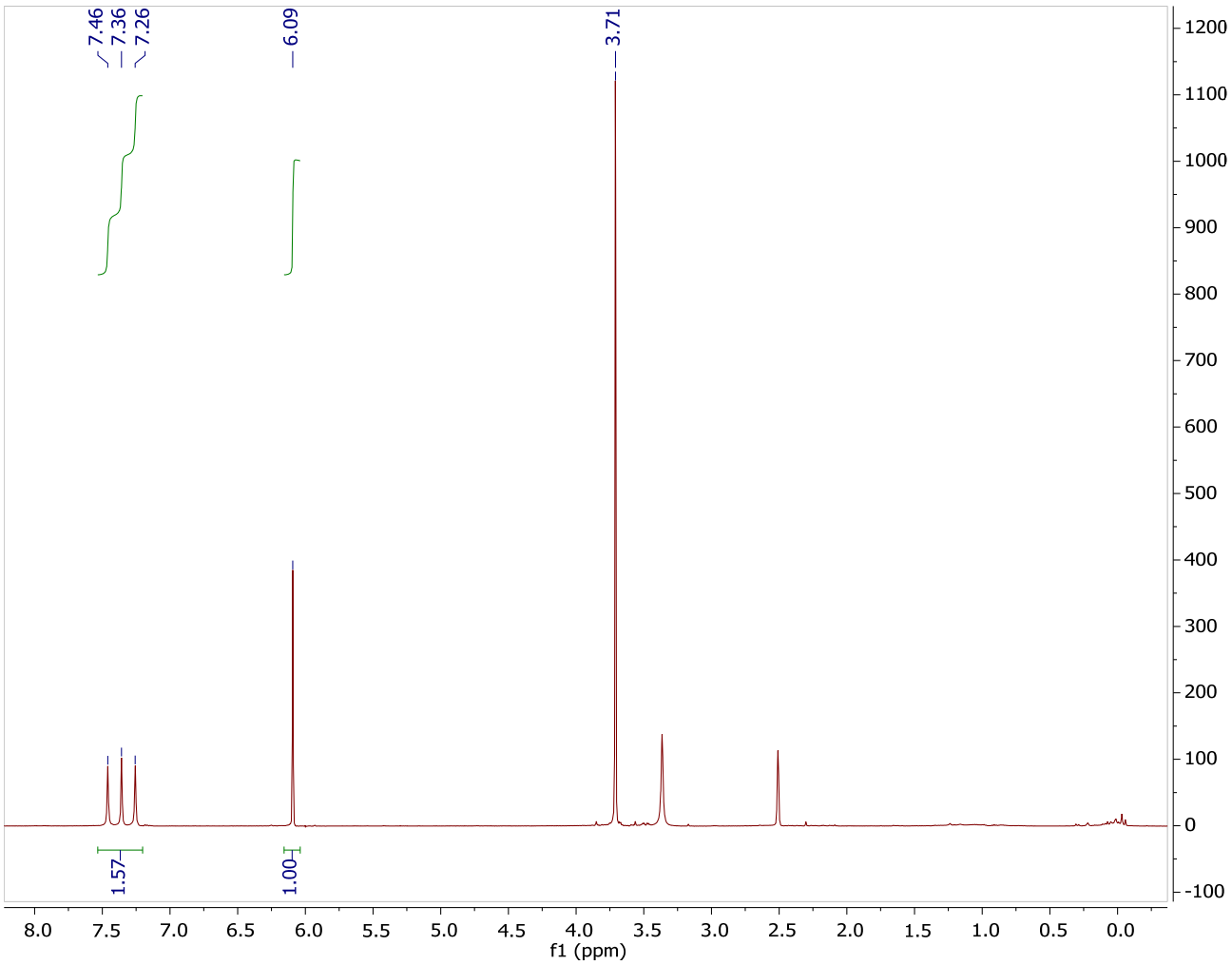

Figure S14. ^{1}H NMR of the reaction between 500 equiv. KC_8 and 500 equiv. Me_3SiCl with 0.2 mol % $Fe_3(\mu_3\text{-}N)$**L** in Et_2O in DMSO-d_6 after HCl quenching.

Peaks at 6.09 and 3.71 ppm indicate 1,3,5-trimethoxybenzene internal standard. $^{1}J_{N\text{-}H}$ = 51 Hz.

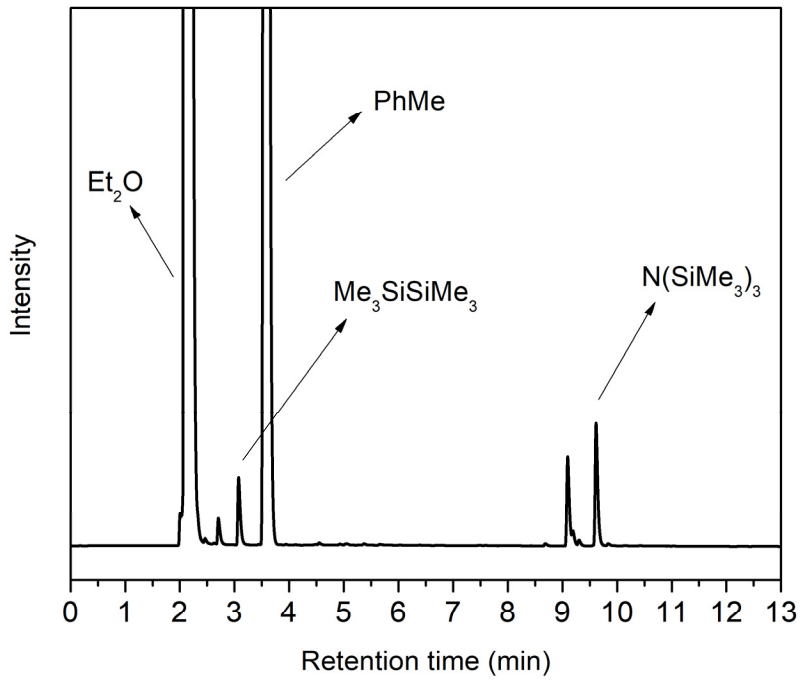

Figure S15. Gas chromatogram of the reaction mixture using 500 equiv. KC_8 and 500 equiv. Me_3SiCl with 0.2 mol % Fe_3Br_3**L** in Et_2O after 24 h.

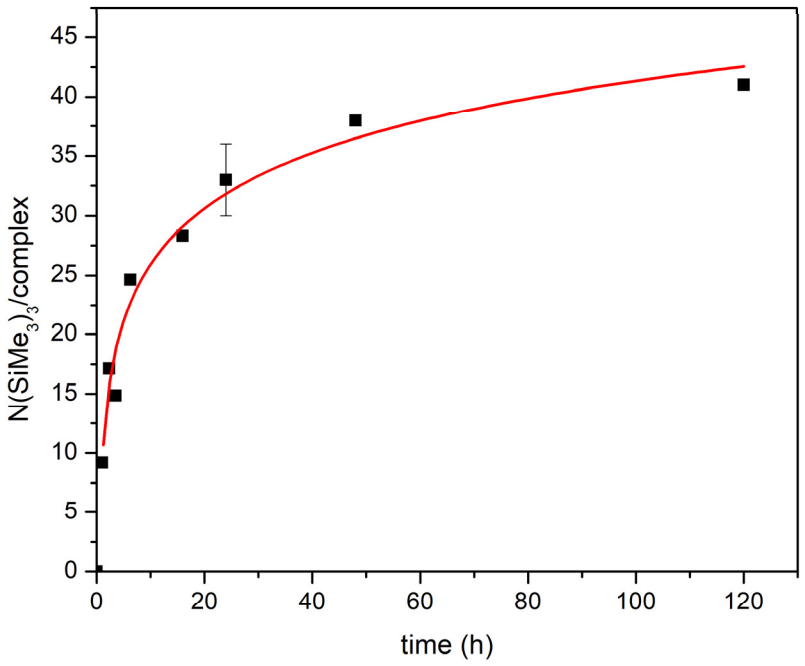

Figure S16. Influence of reaction time on $N(SiMe_3)_3$ production.

The red trend line indicates the fit of the experimental data to a logarithmic growth curve. Reaction conditions: 500 equiv. KC_8 and 500 equiv. Me_3SiCl (0.2 mol% catalyst loading) in toluene at room temperature.

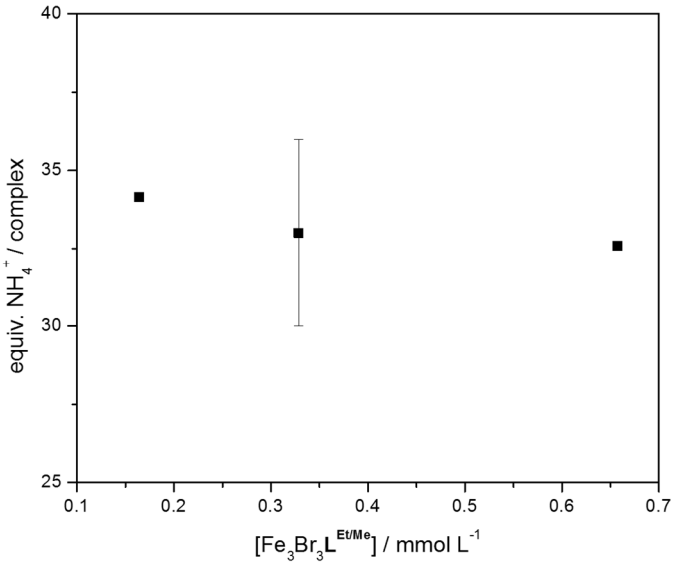

Figure S17. Influence of the concentration of the system on the yield of NH_4^+ obtained using Fe_3Br_3**L**.

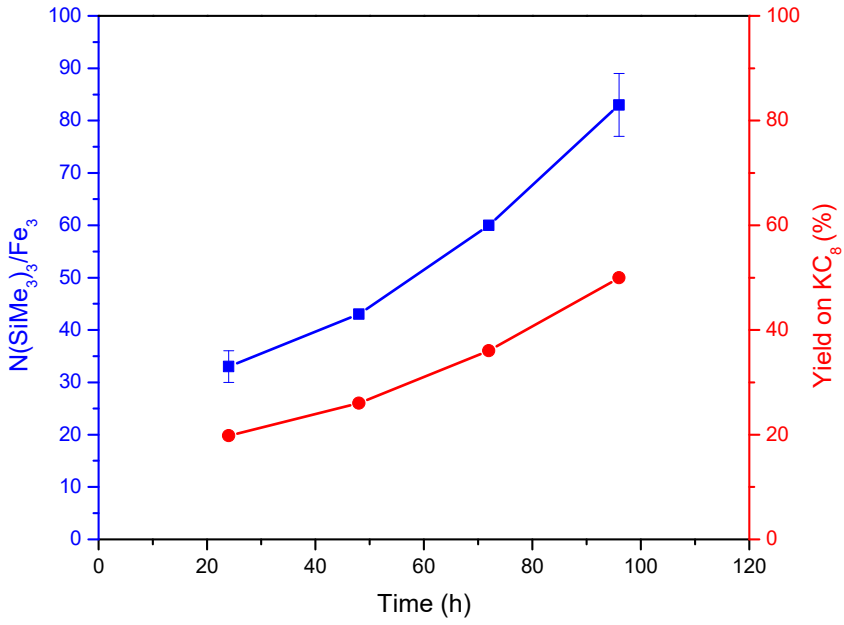

Figure S18. Influence of reaction time on $N(SiMe_3)_3$ production at -34 °C in Et_2O:PhMe = 9:1.

The blue points indicate the value of experimental data of $N(SiMe_3)_3$ equiv. per complex. The red points indicate the corresponding yields based on KC_8. Reaction conditions: 500 equiv. KC_8 and 500 equiv. Me_3SiCl (0.2 mol% catalyst loading) in Et_2O:PhMe = 9:1 at -34 °C.

Table S2. Catalytic performance of reported iron-based complexes for the silylation of N_2.

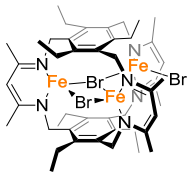

Fe_3Br_3L
This work

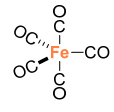

A
Nishibayashi 2012

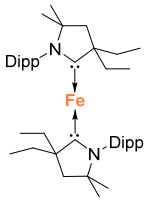

B
Peters 2014

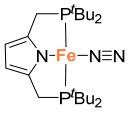

C
Nishibayashi 2016

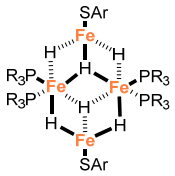

D
Ohki 2017

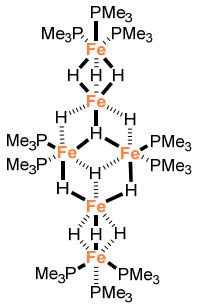

E
Ohki 2017

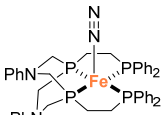

F
Mock 2017

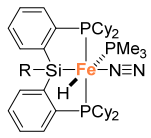

G
Nishibayashi 2017

	Reaction conditions							
Complex	**Solvent**	**PN_2 (atm)**	**Temp.**	**Time (h)**	**KC_8 or Na equiv.**	**NH_4^+ equiv./Fe**	**Yield on KC_8 (%)**	**Ref.**
Fe_3Br_3L	Toluene	1	r. t.	24	500	11	20	*This work*
	Et_2O	1	r. t.	24	500	21	38	
	Et_2O	1	r. t.	24	1800	27	13	
	Et_2O	1	-34 °C	24	500	8	14	
	Et_2O	1	-34 °C	96	500	29	52	
A	THF	1	r. t.	20	600	25	12	7
B	Et_2O	1	r. t.	24	600	24	12	8
	Et_2O	1	-78 °C	24	600	7	3	
C	THF	1	r. t.	20	600	21	10	9
D (PR_3=PMe_3)	DME	1	r. t.	100	2400	31	16	10
D (PR_3=PMe_2Ph)	DME	1	r. t.	100	2400	40	20	
D (PR_3=PEt_3)	DME	1	r. t.	100	2400	40	20	
E	DME	1	r. t.	100	3600	31	15	
	THF	1	r. t.	100	3600	13	6	
F	Toluene	1	r. t.	24	500	11	7	11
	Toluene	20	r. t.	24	500	22	13	
	Toluene	100	r. t.	24	500	38	23	
	Toluene	100	r. t.	24	1000	65	19	
G	THF	1	r. t.	20	600	15	7	12
	THF	1	r. t.	20	600	26	13	

Table S3. Catalytic performance of selected complexes for the silylation of N_2 containing other metals.

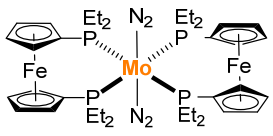

H
Yoshizawa 2011

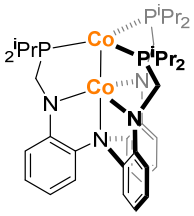

I
Lu 2015

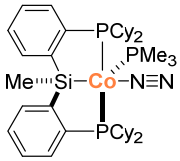

J
Nishibayashi 2017

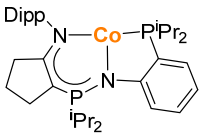

K
Masuda 2018

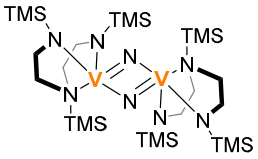

L
Nishibayashi 2017

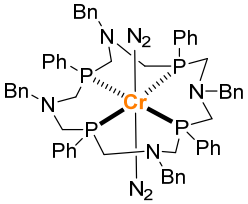

M
Mock 2018

	Reaction conditions							
Complex (M)	**Solvent**	**PN_2 (atm)**	**Temp.**	**Time (h)**	**KC_8 or Na equiv.**	**NH_4^+ equiv./M**	**Yield on KC_8 (%)**	**Ref.**
H (Mo)	THF	1	r. t.	100	4000	150	11	13
	THF	1	r. t.	200	8000	226	8	
I (Co)	THF	1	r. t.	12	2000	97	29	14
	THF	1	r. t.	24	4000	163	24	
J (Co)	THF	1	r. t.	40	600	41	20	12
K (Co)	THF	1	-40 °C	240	1500	200	40	15
	THF	1	-40 °C	312	3000	270	27	
L (V)	THF	1	r. t.	20	600	24	12	16
M (Cr)	THF	1	r. t.	16	100	11	32	17
	THF	1	r. t.	16	100000	17	0.05	
	THF	1	r. t.	72	100000	21	0.06	
	THF	1	r. t.	32	200000	34	0.05	

Reactivity of triiron compounds under reducing conditions

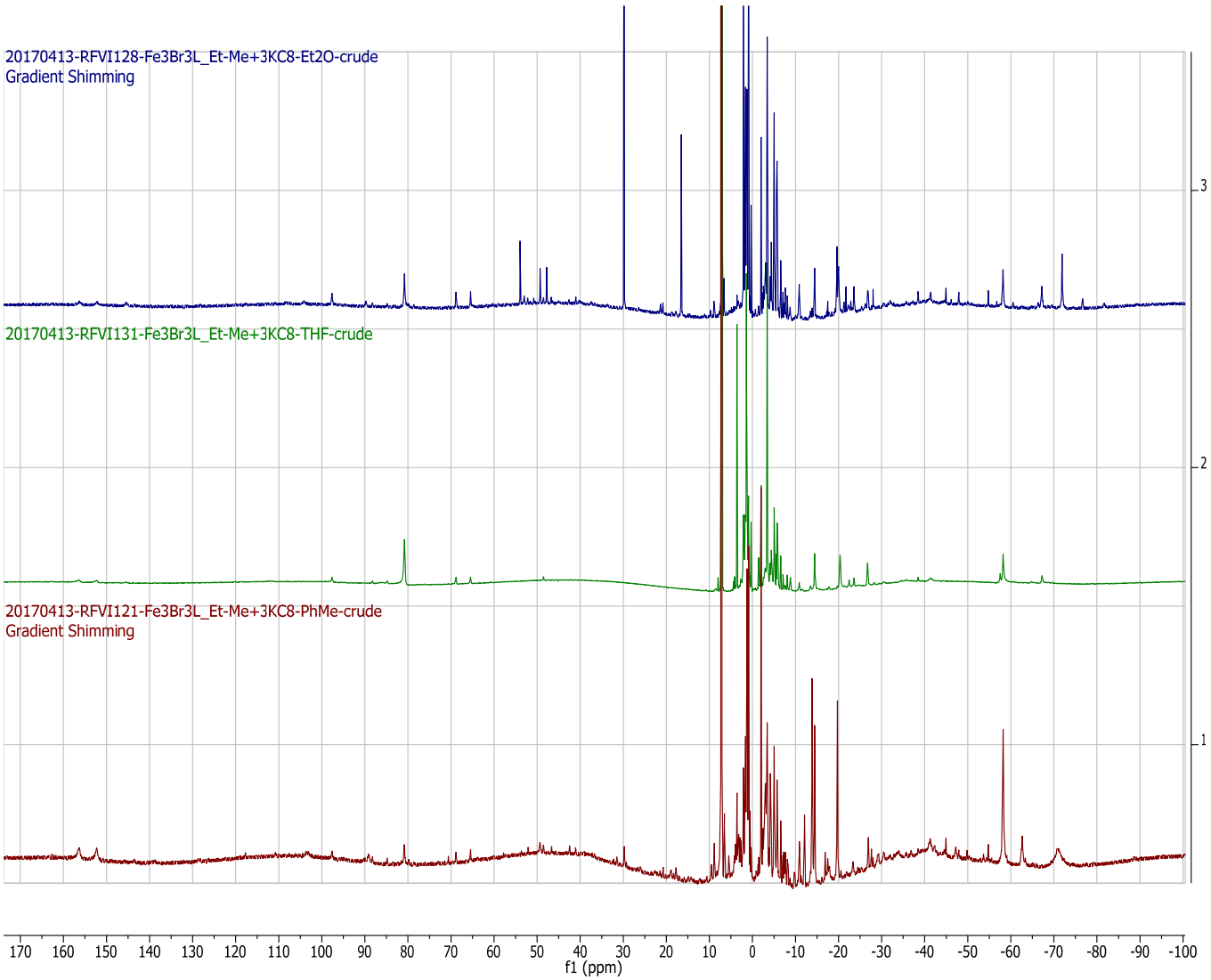

Figure S19. ^{1}H NMR spectra in C_6D_6 of Fe_3Br_3**L** with 3 equiv. of KC_8 in toluene (bottom), THF (middle), and Et_2O (top).

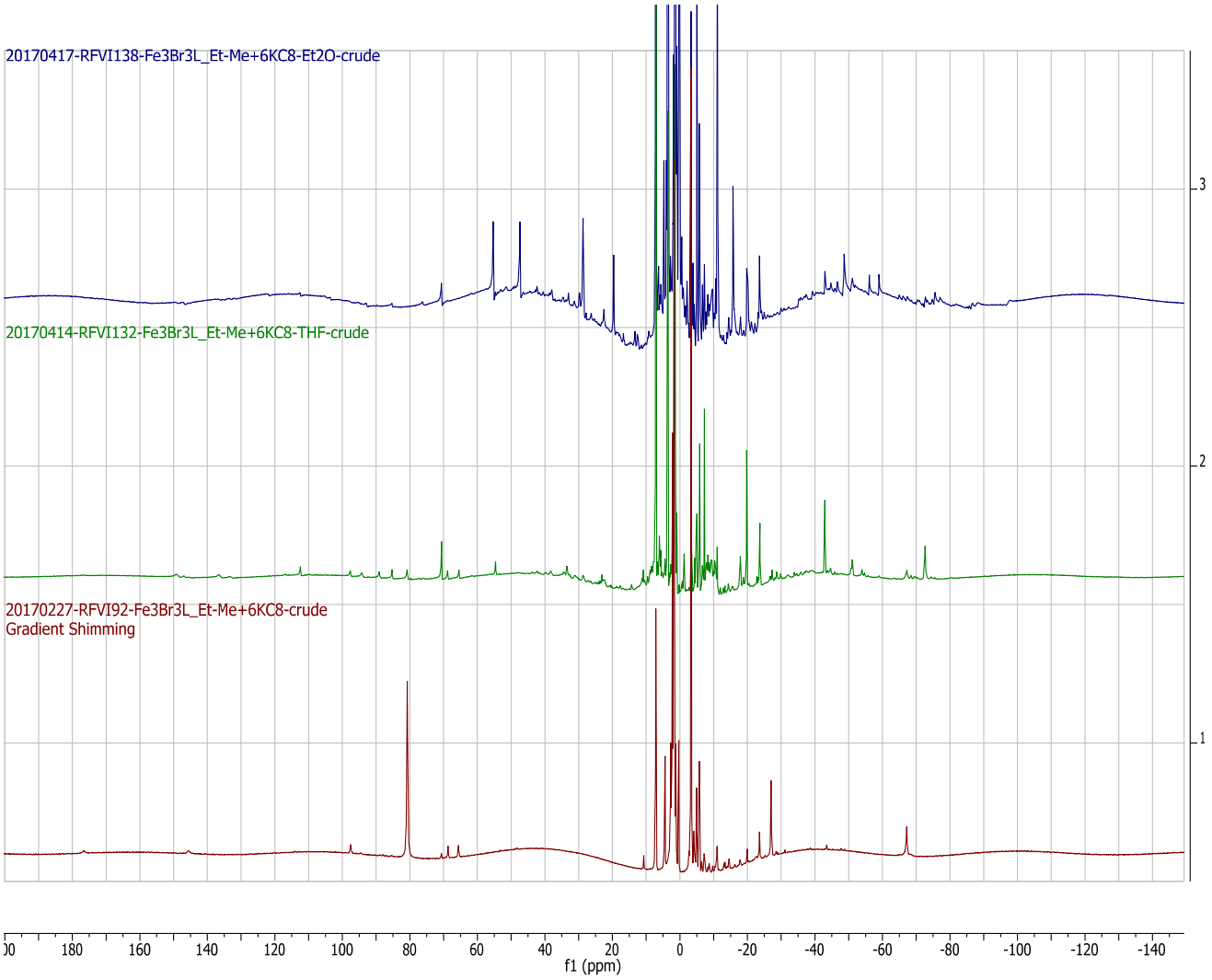

Figure S20. ^{1}H NMR spectra in C_6D_6 of Fe_3Br_3**L** with 6 equiv. of KC_8 in toluene (bottom), THF (middle), and Et_2O (top).

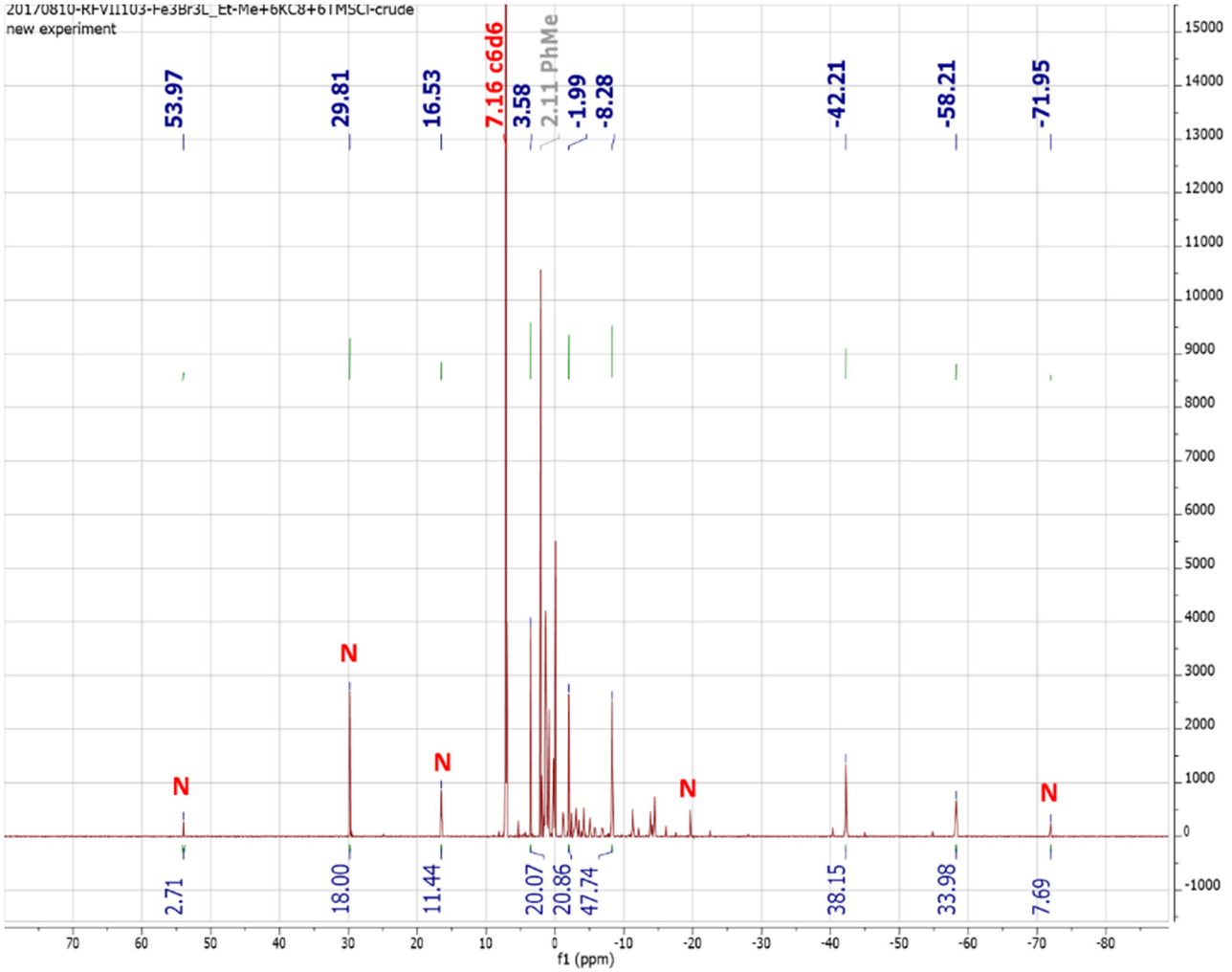

Figure S21. ^{1}H NMR spectra in C_6D_6 of Fe_3Br_3**L** with 6 equiv. of KC_8 and Me_3SiCl in toluene at 25 °C after 24 h. The peaks indicated with N are assigned to $Fe_3(\mu_3\text{-N})$L.

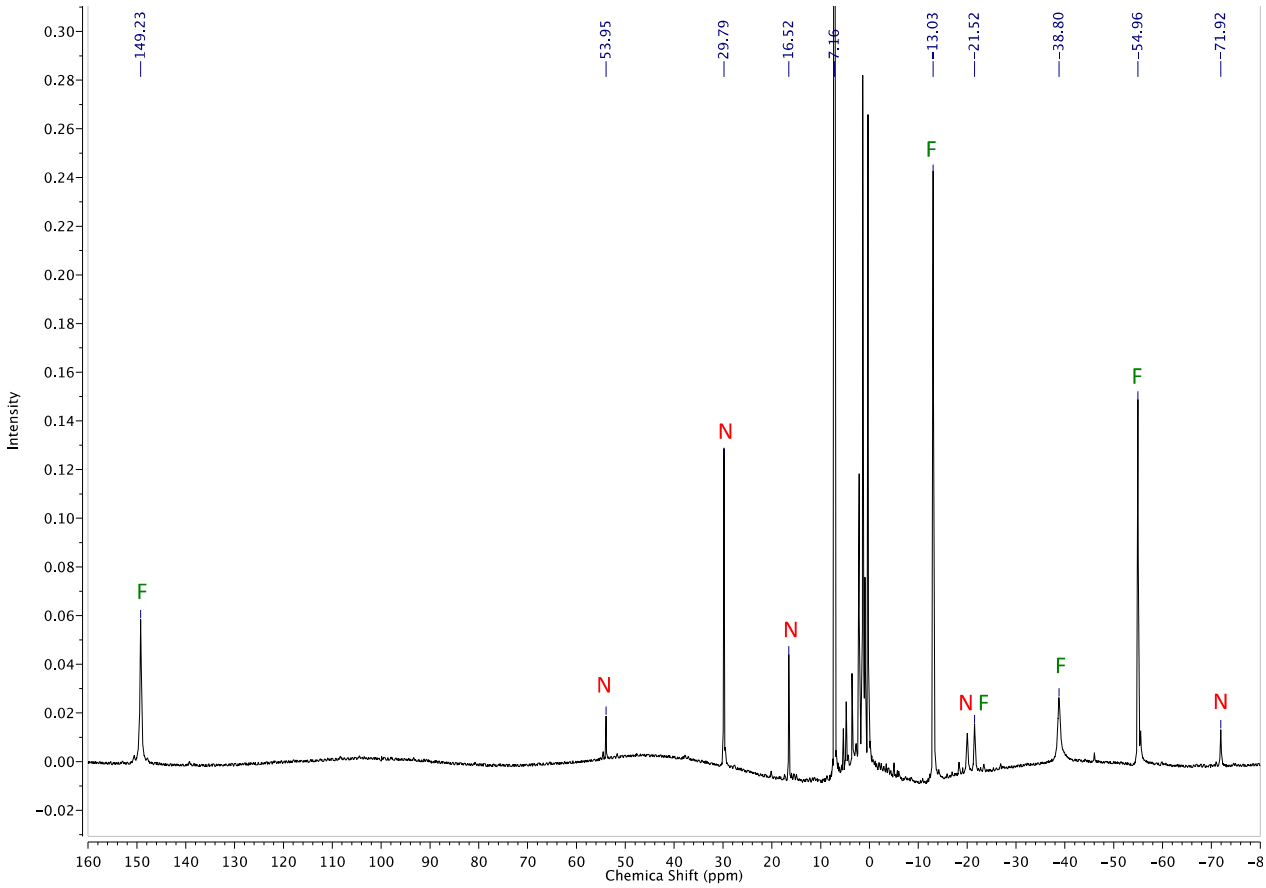

Figure S22. ^{1}H NMR spectra in C_6D_6 of Fe_3F_3**L** with 6 equiv. of KC_8 and 6 equiv Me_3SiCl in toluene at 25 °C after 24 h.

The peaks indicated with **F** and **N** are assigned to $Fe_3(\mu_3\text{-}N)$**L**.

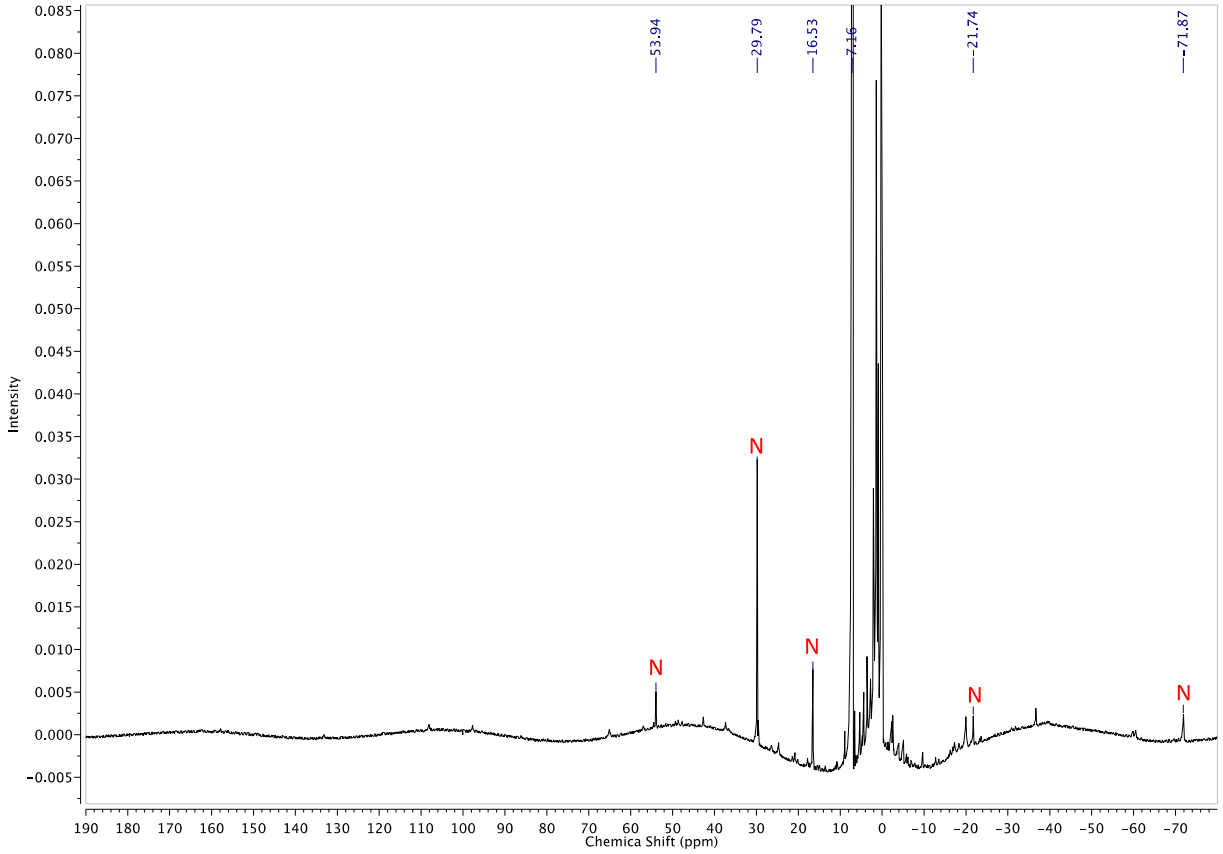

Figure S23. ^{1}H NMR spectra in C_6D_6 of Fe_3Cl_3**L** with 6 equiv. of KC_8 and 6 equiv. of Me_3SiCl in toluene at 25 °C after 24 h.

The peaks indicated with **N** are assigned to $Fe_3(\mu_3\text{-}N)$**L**.

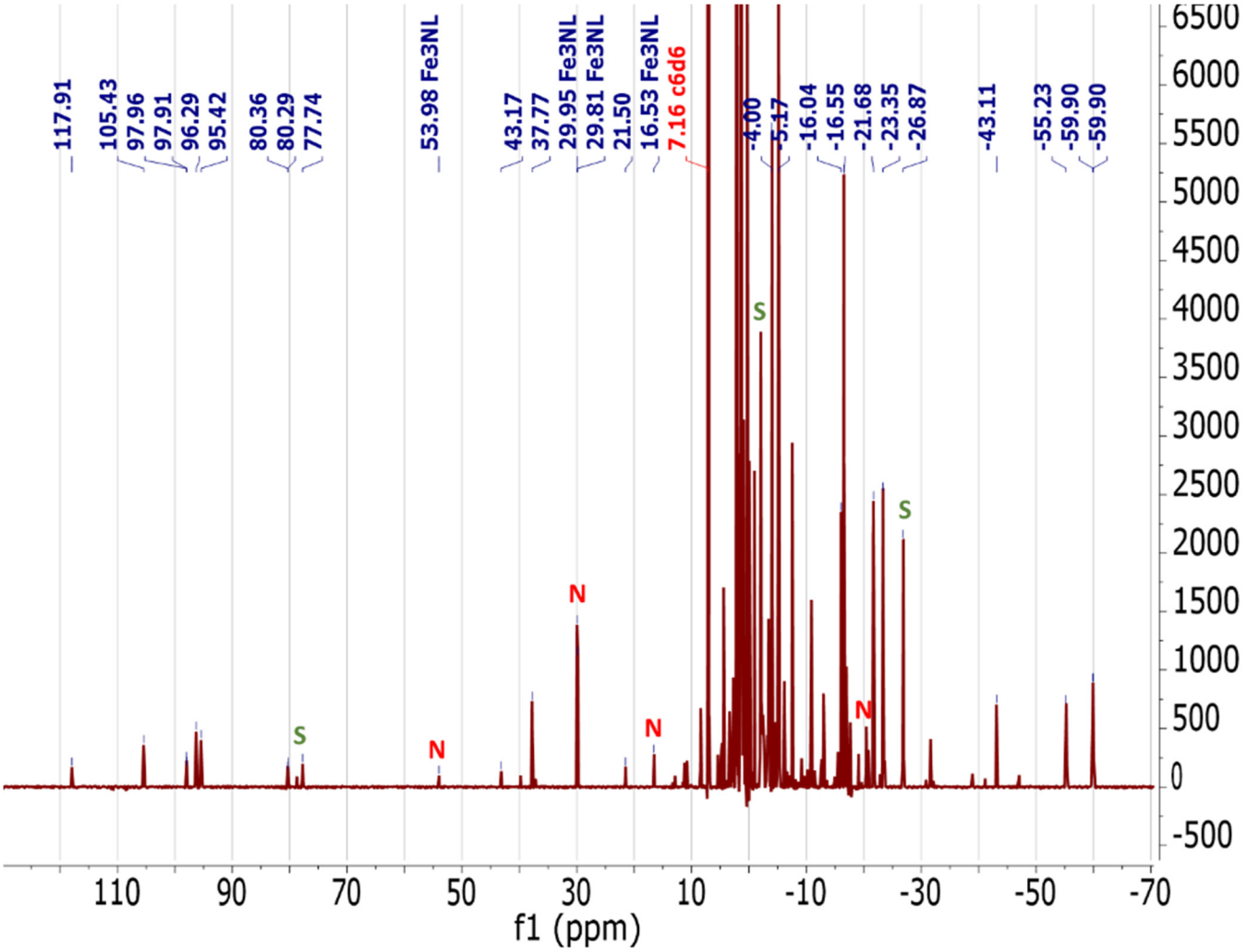

Figure S24. ^{1}H NMR spectra in C_6D_6 of Fe_3S_3**L** with 6 equiv. of KC_8 and 6 equiv. of Me_3SiCl in toluene at 25 °C after 24 h.

The peaks indicated with **S** and **N** are assigned to Fe_3S_3**L** and $Fe_3(\mu_3\text{-N})$**L**, respectively.

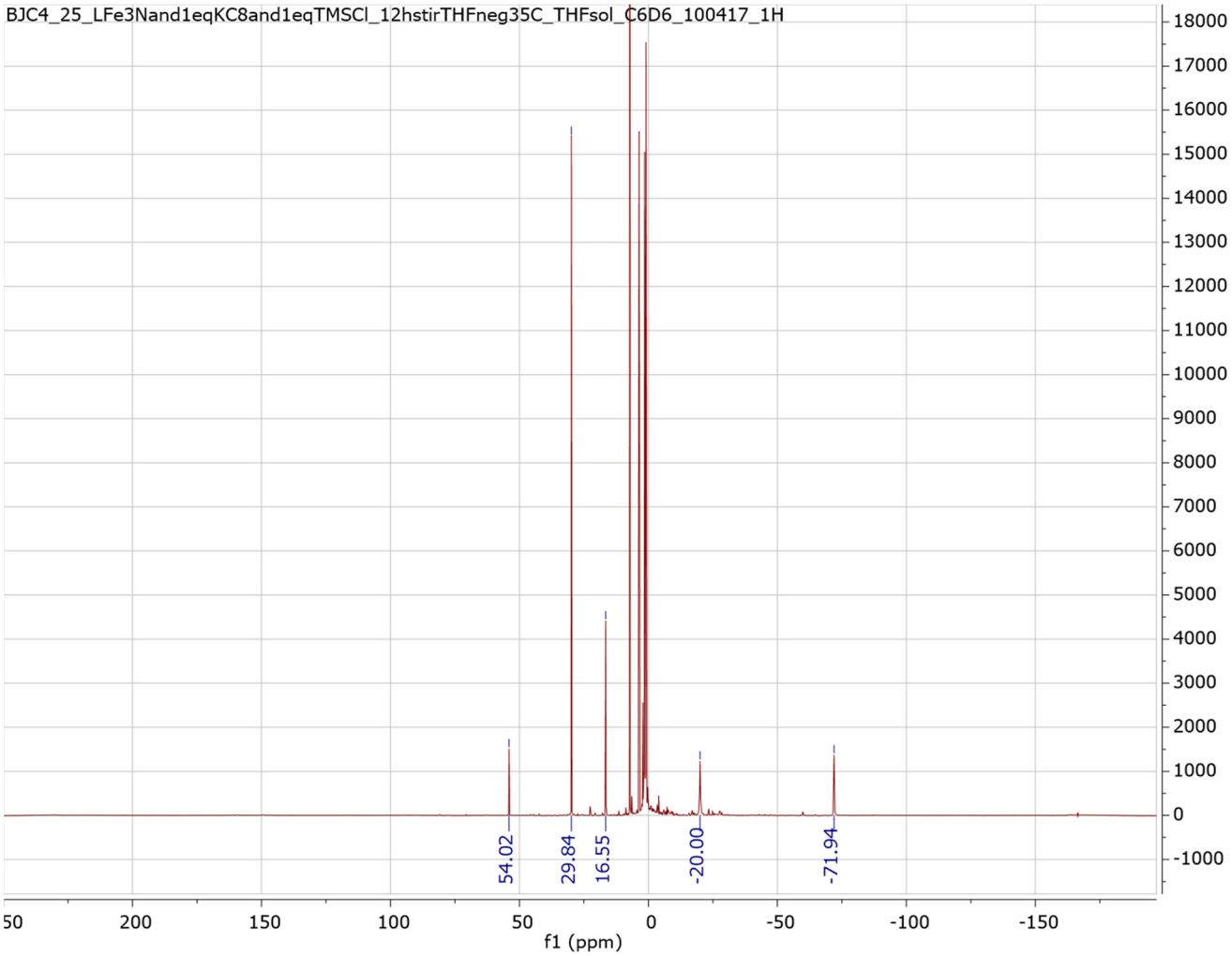

Figure S25. ^{1}H NMR of the reaction between $Fe_3(\mu_3\text{-}N)$**L**, 1 equiv. KC_8 and 1 equiv. Me_3SiCl in THF at −35 °C recorded in C_6D_6.

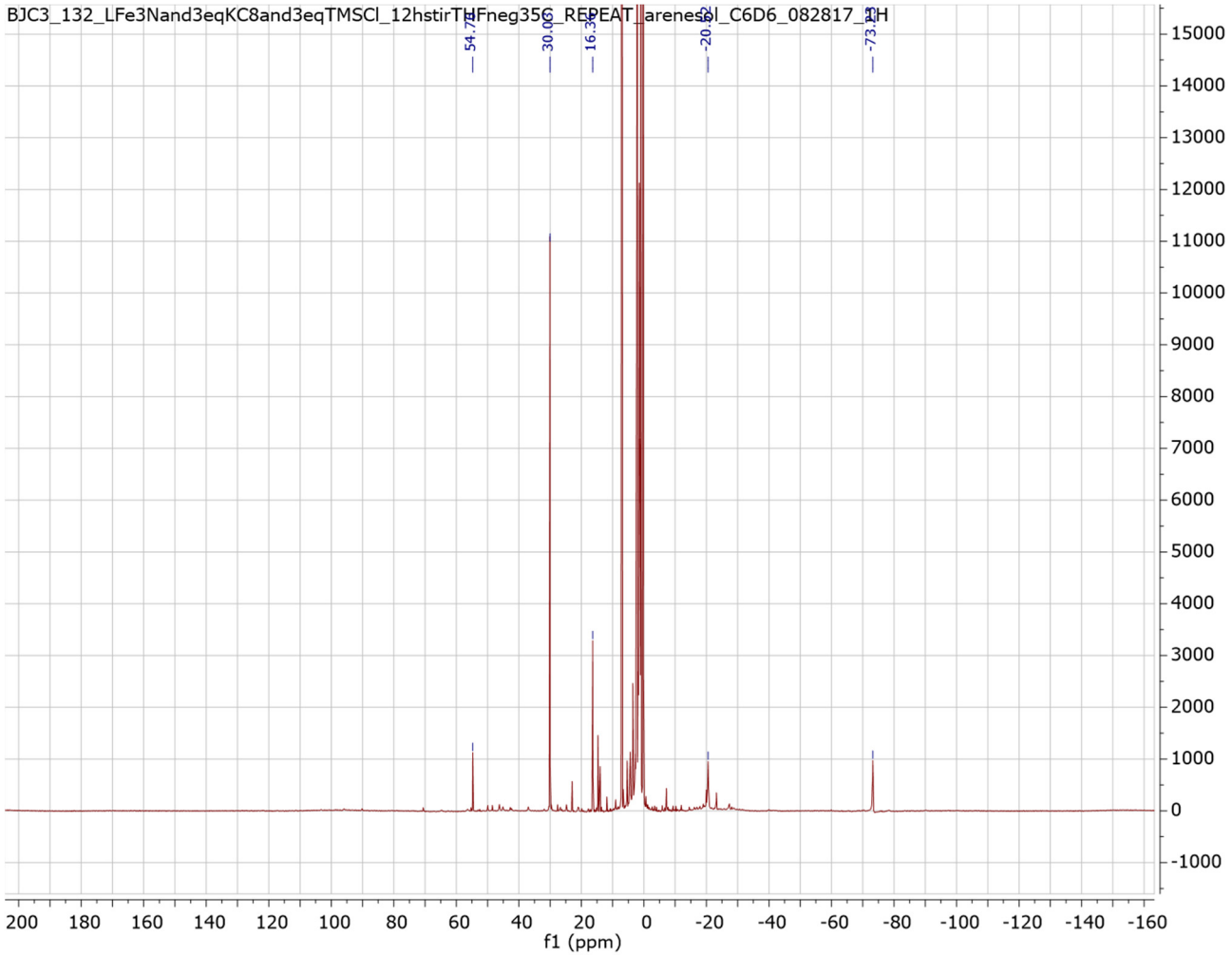

Figure S26. ^{1}H NMR of the reaction between $Fe_3(\mu_3\text{-}N)$**L**, 3 equiv. KC_8 and 3 equiv. Me_3SiCl in THF at −35 °C recorded in C_6D_6.

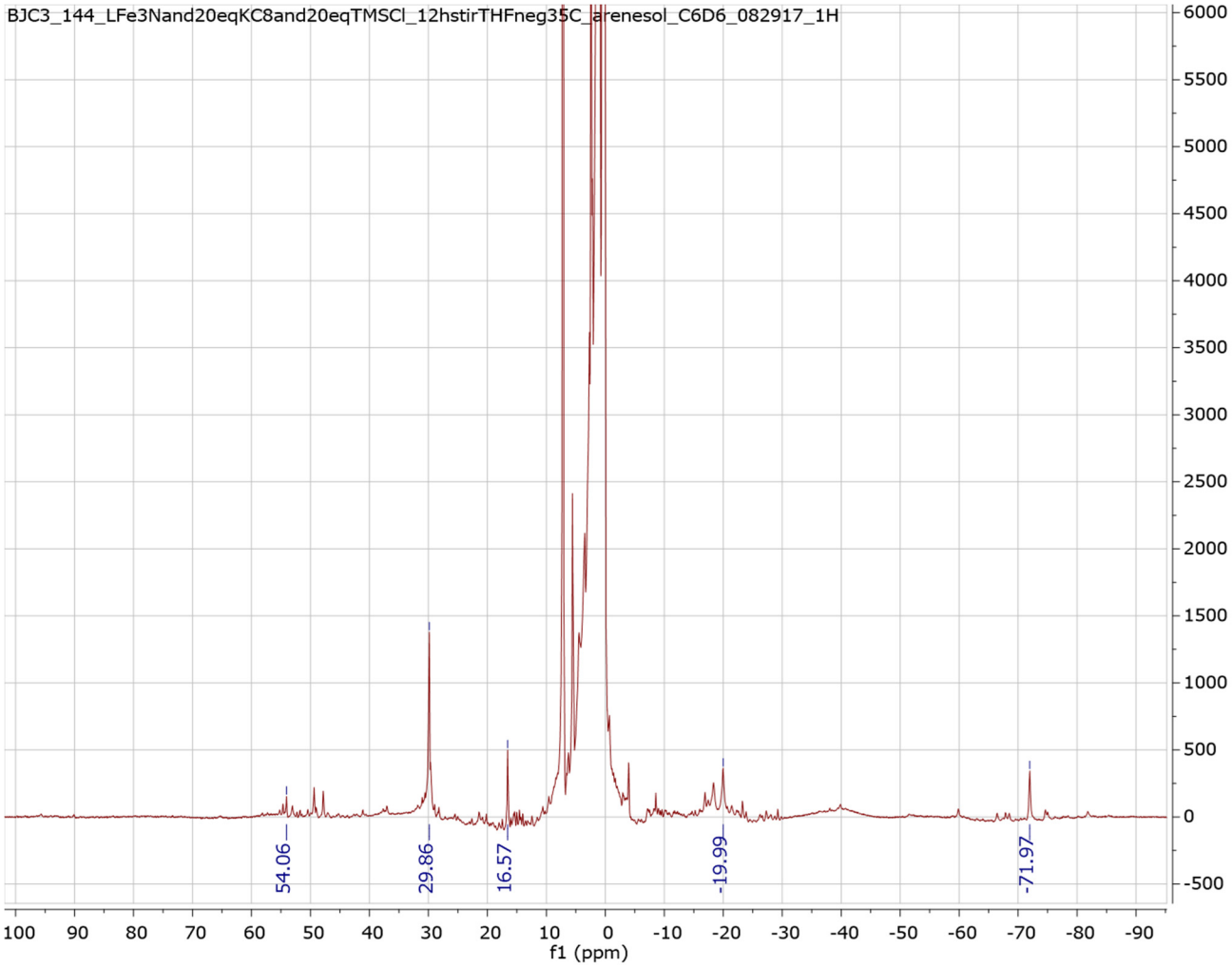

Figure S27. ^{1}H NMR of the reaction between $Fe_3(\mu_3\text{-}N)L$, 20 equiv. KC_8 and 20 equiv. Me_3SiCl in THF at –35 °C recorded in C_6D_6.

Crystallographic data

Table S4. Crystal data for Fe_3Cl_3**L**.

Identification code	bk102a_0m	
Empirical formula	C57 H75 Cl3 Fe3 N6	
Formula weight	1118.13	
Temperature	100(2) K	
Wavelength	0.71073 Å	
Crystal system	Triclinic	
Space group	P-1	
Unit cell dimensions	a = 12.6922(5) Å	a= 76.0639(7)°.
	b = 13.0313(5) Å	b= 84.1498(7)°.
	c = 16.6470(6) Å	g = 84.0536(7)°.
Volume	2649.46(17) $Å^3$	
Z	2	
Density (calculated)	1.402 Mg/m^3	
Absorption coefficient	1.006 mm^{-1}	
F(000)	1176	
Crystal size	0.138 x 0.130 x 0.088 mm^3	
Theta range for data collection	1.264 to 29.999°.	
Index ranges	-17<=h<=17, -18<=k<=18, -23<=l<=23	
Reflections collected	65920	
Independent reflections	15433 [R(int) = 0.0897]	
Completeness to theta = 25.242°	100.0 %	
Absorption correction	None	
Refinement method	Full-matrix least-squares on F^2	
Data / restraints / parameters	15433 / 0 / 634	
Goodness-of-fit on F^2	1.002	
Final R indices [I>2sigma(I)]	R1 = 0.0570, wR2 = 0.1025	
R indices (all data)	R1 = 0.1038, wR2 = 0.1130	
Extinction coefficient	n/a	
Largest diff. peak and hole	1.491 and -0.876 $e.Å^{-3}$	

References

(1) Guillet, G. L.; Sloane, F. T.; Ermert, D. M.; Calkins, M. W.; Peprah, M. K.; Knowles, E. S.; Čižmár, E.; Abboud, K. A.; Meisel, M. W.; Murray, L. J. Preorganized Assembly of Three Iron(II) or Manganese(II) β-Diketiminate Complexes Using a Cyclophane Ligand. *Chem. Commun.* **2013**, *49*, 6635–6637.

(2) Ermert, D. M.; Gordon, J. B.; Abboud, K. A.; Murray, L. J. Nitride-Bridged Triiron Complex and Its Relevance to Dinitrogen Activation. *Inorg. Chem.* **2015**, *54*, 9282–9289.

(3) Lee, Y.; Anderton, K. J.; Sloane, F. T.; Ermert, D. M.; Abboud, K. A.; García-Serres, R.; Murray, L. J. Reactivity of Hydride Bridges in High-Spin [3M–3(μ-H)] Clusters (M = Fe^{II}, Co^{II}). *J. Am. Chem. Soc.* **2015**, *3*, 10610–10617.

(4) Lee, Y.; Abboud, K. A.; García-Serres, R.; Murray, L. J. A Three-Coordinate Fe(II) Center within a [3Fe–(μ_3-S)] Cluster That Provides an Accessible Coordination Site. *Chem. Commun.* **2016**, *52*, 9295–9298.

(5) Anderton, K. J.; Knight, B. J.; Rheingold, A. L.; Abboud, K. A.; García-Serres, R.; Murray, L. J. Reactivity of Hydride Bridges in a High-Spin $[Fe_3(\mu\text{-}H)_3]^{3+}$ Cluster: Reversible H_2/CO Exchange and Fe–H/B–F Bond Metathesis. *Chem. Sci.* **2017**, *8*, 4123–4129.

(6) Eckert, N. A.; Smith, J. M.; Lachicotte, R. J.; Holland, P. L. Low-Coordinate Iron(II) Amido Complexes of β-Diketiminates: Synthesis, Structure, and Reactivity. *Inorg. Chem.* **2004**, *43*, 3306–3321.

(7) Yuki, M.; Tanaka, H.; Sasaki, K.; Miyake, Y.; Yoshizawa, K.; Nishibayashi, Y. Iron-Catalysed Transformation of Molecular Dinitrogen into Silylamine under Ambient Conditions. *Nat. Commun.* **2012**, *3*, 1254.

(8) Ung, G.; Peters, J. C. Low-Temperature N_2 Binding to Two-Coordinate L_2Fe^0 Enables Reductive Trapping of $L_2FeN_2^-$ and NH_3 Generation. *Angew. Chem. Int. Ed.* **2015**, *54*, 532–535.

(9) Kuriyama, S.; Arashiba, K.; Nakajima, K.; Matsuo, Y.; Tanaka, H.; Ishii, K.; Yoshizawa, K.; Nishibayashi, Y. Catalytic Transformation of Dinitrogen into Ammonia and Hydrazine by Iron-Dinitrogen Complexes Bearing Pincer Ligand. *Nat. Commun.* **2016**, *7*, 12181.

(10) Araake, R.; Sakadani, K.; Tada, M.; Sakai, Y.; Ohki, Y. [Fe_4] and [Fe_6] Hydride Clusters Supported by Phosphines: Synthesis, Characterization, and Application in N_2 Reduction. *J. Am. Chem. Soc.* **2017**, *139*, 5596–5606.

(11) Prokopchuk, D. E.; Wiedner, E. S.; Walter, E. D.; Popescu, C. V.; Piro, N. A.; Kassel, W. S.; Bullock, R. M.; Mock, M. T. Catalytic N_2 Reduction to Silylamines and Thermodynamics of N_2 Binding at Square Planar Fe. *J. Am. Chem. Soc.* **2017**, *139*, 9291–9301.

(12) Imayoshi, R.; Nakajima, K.; Takaya, J.; Iwasawa, N.; Nishibayashi, Y. Synthesis and Reactivity of Iron- and Cobalt-Dinitrogen Complexes Bearing PSiP-Type Pincer Ligands toward Nitrogen Fixation. *Eur. J. Inorg. Chem.* **2017**, *2017*, 3769–3778.

(13) Tanaka, H.; Sasada, A.; Kouno, T.; Yuki, M.; Miyake, Y.; Nakanishi, H.; Nishibayashi, Y.; Yoshizawa, K. Molybdenum-Catalyzed Transformation of Molecular Dinitrogen into Silylamine: Experimental and DFT Study on the Remarkable Role of Ferrocenyldiphosphine Ligands. *J. Am. Chem. Soc.* **2011**, *133*, 3498–3506.

(14) Siedschlag, R. B.; Bernales, V.; Vogiatzis, K. D.; Planas, N.; Clouston, L. J.; Bill, E.; Gagliardi, L.; Lu, C. C. Catalytic Silylation of Dinitrogen with a Dicobalt Complex. *J. Am. Chem. Soc.* **2015**, *137*, 4638–4641.

(15) Suzuki, T.; Fujimoto, K.; Takemoto, Y.; Wasada-Tsutsui, Y.; Ozawa, T.; Inomata, T.; Fryzuk, M. D.;

Masuda, H. Efficient Catalytic Conversion of Dinitrogen to $N(SiMe_3)_3$ Using a Homogeneous Mononuclear Cobalt Complex. *ACS Catal.* **2018**, *8*, 3011–3015.

(16) Imayoshi, R.; Nakajima, K.; Nishibayashi, Y. Vanadium-Catalyzed Reduction of Molecular Dinitrogen into Silylamine under Ambient Reaction Conditions. *Chem. Lett.* **2017**, *46*, 466–468.

(17) Kendall, A. J.; Johnson, S. I.; Bullock, R. M.; Mock, M. T. Catalytic Silylation of N 2 and Synthesis of NH 3 and N 2 H 4 by Net Hydrogen Atom Transfer Reactions Using a Chromium P 4 Macrocycle. *J. Am. Chem. Soc.* **2018**, *140*, 2528–2536.